Archives of Biochemistry and Biophysics
Vol. 362, No. 2, February 15, pp. 254–264, 1999
Article ID abbi.1998.1035, available online at http://www.idealibrary.com on IDEAL®

Properties of the His^{57}–Asp^{102} Dyad of Rat Trypsin D189S in the Zymogen, Activated Enzyme, and α_1-Proteinase Inhibitor Complexed Forms

Gyula Kaslik,* William M. Westler,* László Gráf,† and John L. Markley*,[1]

Department of Biochemistry and National Magnetic Resonance Facility at Madison, University of Wisconsin-Madison, Madison, Wisconsin 53706; and †Department of Biochemistry, Eötvös University, H-1088 Puskin u. 3, Budapest, Hungary

Received August 28, 1998, and in revised form October 20, 1998

Structural and biochemical studies suggest that serpins induce structural rearrangements in their target serine-proteinases. Previous NMR studies of the complex between a serpin, α_1-proteinase inhibitor, and a mutant of recombinant rat trypsin (the Asp^{189} to Ser mutant, D189S, which is much more stable than wild-type rat trypsin against autoproteolysis) provided information about the state of catalytic residues in this complex: the hydrogen bond between Asp^{102} and His^{57} remains intact in the complex, and spectral properties of His^{57} are more like those of the zymogen than of the activated enzyme (G. Kaslik, *et al.*, 1997, *Biochemistry* 36, 5455–5464). Here we report the protonation and exchange behavior of His^{57} of recombinant rat trypsin D189S in three states: the zymogen, the active enzyme, and the complex with human α_1-proteinase inhibitor and compare these with analogous behavior of His^{57} of bovine chymotrypsinogen and α-chymotrypsin. In these studies the pK_a of His^{57} has been determined from the pH dependence of the ^{1}H NMR signal from the H$^{\delta 1}$ proton of histidine in the Asp^{102}–His^{57} dyad, and a measure of the accessibility of this part of the active site has been obtained from the rate of appearance of this signal following its selective saturation. The activation of rat trypsinogen D189S (zymogen, pK_a = 7.8 ± 0.1; Hill coefficient = 0.86 ± 0.05) decreased the pK_a of His^{57} by 1.1 unit and made the protonation process cooperative (active enzyme, pK_a = 6.7 ± 0.1; Hill coefficient = 1.37 ± 0.08). The binding of α_1-proteinase inhibitor to trypsin D189S led to an increase in the pK_a value of His^{57} to a value higher than that of the zymogen and led to negative cooperativity in the protonation process (complex, pK_a = 8.1 ± 0.1; Hill coefficient = 0.70 ± 0.08), as was observed for the zymogen. In spite of these differences in the pK_a of His^{57} in the zymogen, active enzyme, and α_1-proteinase inhibitor complex, the solvent exchange lifetime of the His^{57} H$^{\delta 1}$ proton was the same, within experimental error, in all three states (lifetime = 2 to 12.5 ms). The linewidth of the ^{1}H NMR signal from the H$^{\delta 1}$ proton of His^{57} was relatively sharp, at temperatures between 5 and 20°C at both low pH (5.2) and high pH (10.0), in spectra of bovine α-chymotrypsin, recombinant rat trypsin D189S, and the complex between rat trypsin D189S and human α_1-proteinase inhibitor; however, in spectra of the complex between α-chymotrypsin and human α_1-proteinase inhibitor, the peak was broader and could be well-resolved only at the lower temperature (5°C).

Key Words: **serine-proteases; serpin; active site; NMR.**

The canonical protein inhibitors of serine proteinases are thought to bind by a classical lock and key mechanism in which a rigid inhibitor binds to the rigid active site of the cognate proteinase (1). The most stable form of the complex is one that resembles a Michaelis complex prior to any chemical attack or cleavage (2, 3), although the mechanism for stabilization of this stage of the reaction in the complex has not been explained in full detail. The region of the inhibitor that interacts with the proteinase, the reactive site loop, may show some flexibility in solution, but this is usually interpreted as a hinge motion of a relatively rigid loop (4, 5).

Members of the serpin subfamily of serine proteinase inhibitors inhibit their target proteinases in a different

[1] To whom correspondence should be addressed: Department of Biochemistry, University of Wisconsin–Madison, 433 Babcock Drive, Madison, WI 53706. Fax: (608) 262-3453. E-mail: markley@nmrfam.wisc.edu.

0003-9861/99 $30.00

manner. A body of work suggests that serpins stabilize the acyl-enzyme intermediate stage of the proteolytic reaction (6–10). Although structures of both intact and proteolytically modified serpins have been solved by X-ray crystallography, no structure of a serpin:proteinase complex is available, and it is unclear how the serpins achieve the stabilization of what otherwise is a short-lived acyl-enzyme intermediate. In addition, the reactive-site loop of an active serpin (residues $\sim P_{15}$–P_5' in the Schecter–Berger (11) notation, where P_1 is the reactive site residue and unprimed residues with increasing numbers are toward the N-terminus and primed residues are toward the C-terminus) can adopt remarkably variable structural rearrangements (12–17). This suggests that the reactive-site loops of serpins are considerably more flexible than those of canonical serine proteinase inhibitors (18). Whereas reactive-site cleavage in canonical serine proteinase inhibitors leads to no major structural perturbation and is reversible, with the cleaved form active as an inhibitor (1), reactive-site cleavage in serpins leads to a dramatic structural rearrangement and attendant irreversible inactivation of the inhibitor. Following cleavage, the P_1 and P_1' residues become separated by ~70 Å and located on opposite sides of the serpin molecule (19–22), and the P_{14}–P_1 part of the reactive-site loop has migrated and become inserted into the five-stranded antiparallel β-sheet-A (10, 23).

The structure of the proteinase also is altered in the serpin:proteinase complex. Evidence for this comes from enhanced susceptibility to limited proteolysis (7, 24) and disulfide reduction (25). These results indicate that complex formation with serpin causes certain parts of the proteinase to become more accessible to proteolytic attack and more "open" to the reducing agent. It is worth noting, however, that in spite of the localized increase in structural flexibility, the global heat stability of trypsin D189S was found to be remarkably higher in the complex than in the enzyme alone (25). On the basis of ^{1}H NMR investigations of the complex between bovine chymotrypsin and a recombinant human α_1-antichymotrypsin variant, it was suggested that the structural rearrangement disrupts the hydrogen bond between Asp^{102} and His^{57} of the serine proteinase (26) and that this accounts for the stability of the acyl-enzyme intermediate. However, a subsequent ^{1}H NMR study of two other complexes, recombinant rat trypsin–α_1-proteinase inhibitor and rat trypsin D189S–α_1-proteinase inhibitor (25), provided evidence that the hydrogen bond between Asp^{102} and His^{57} of the serine proteinase is intact in these complexes. The latter results suggested further that the plastic activation domain of the proteinase, which is involved in the structural rearrangement that accompanies zymogen activation (27), plays a crucial role in the serpin-induced structural rearrangement (25) and that serpin binding induces a zymogen-like structure that would account for the catalytic inactivation (25). The D189S mutant was used in this study because of its much lower rate of autoproteolysis compared to wild-type rat trypsin. Both wild-type rat trypsin and its D189S mutant were found to form stable complexes with α_1-proteinase inhibitor, and both exhibited similar NMR spectra (25).

The aims of the present study were *first* to determine accurate values for the pK_a of His^{57} in three forms of recombinant rat trypsin D189S (the zymogen, active enzyme, and α_1-proteinase inhibitor complexed forms) and *second* to investigate whether the hydrogen bond between Asp^{102} and His^{57} remains intact in the complex between α_1-proteinase inhibitor and α-chymotrypsin. The unique high-frequency ^{1}H NMR signal from the proton hydrogen bonded between Asp^{102} and His^{57} (28–30) provided the probe for these investigations. Previous ^{1}H NMR studies of the activation of porcine trypsinogen (31) and bovine chymotrypsinogen (32) had shown that the pK_a value of His^{57} is higher in the zymogens than in the active enzymes.

As predicted by the proposed zymogen-like structure for the serpin complexes, the results reported here show that the pK_a value of His^{57} in rat trypsinogen D189S (zymogen pK_a = 7.8) is similar to that in the trypsin D189S–α_1-proteinase inhibitor complex (complex pK_a = 8.1) and that both are significantly higher than in rat trypsin D189S (active enzyme pK_a = 6.7). The Hill coefficients for the pH titration curves of the zymogen (n = 0.86) and complex (n = 0.70) indicated negative cooperativity for proton binding, whereas that for the active enzyme (n = 1.37) indicated positive cooperativity. In the bovine α-chymotrypsin–human α_1-proteinase inhibitor complex, the proton hydrogen bonded between His^{57} and Asp^{102} yielded a broad signal at 5°C but not at 20°C, both at low pH (chemical shift δ_{DSS} = 18 ppm at pH 5.2) and at high pH (chemical shift δ_{DSS} = 14.8 ppm at pH 10.0). By contrast, sharp signals attributed to this hydrogen-bonded proton were observable at both high and low pH at both temperatures (5°C but not at 20°C) in ^{1}H NMR spectra of the other proteins and complexes studied: bovine chymotrypsinogen, rat trypsin D189S, and the complexes of each of these with human α_1-proteinase inhibitor.

MATERIALS AND METHODS

Materials. Bovine chymotrypsinogen A, bovine α-chymotrypsin A_α, and human α_1-proteinase inhibitor were purchased from Sigma (St. Louis, MO). Human α_1-proteinase inhibitor was dissolved in 0.1 M potassium phosphate buffer, pH 7.0, and was purified on a column containing concanavalin A–Sepharose 4B (Sigma) and eluted with 0.1 M glucose dissolved in the same buffer. After dialysis against 20 mM potassium phosphate buffer, pH 7.6, the sample was loaded onto a column of QAE–Sephacell (Pharmacia, Uppsala, Sweden); the column was eluted with a linear gradient from 0 to 0.5 M NaCl in 20 mM potassium phosphate buffer, pH 7.6. Fractions were monitored

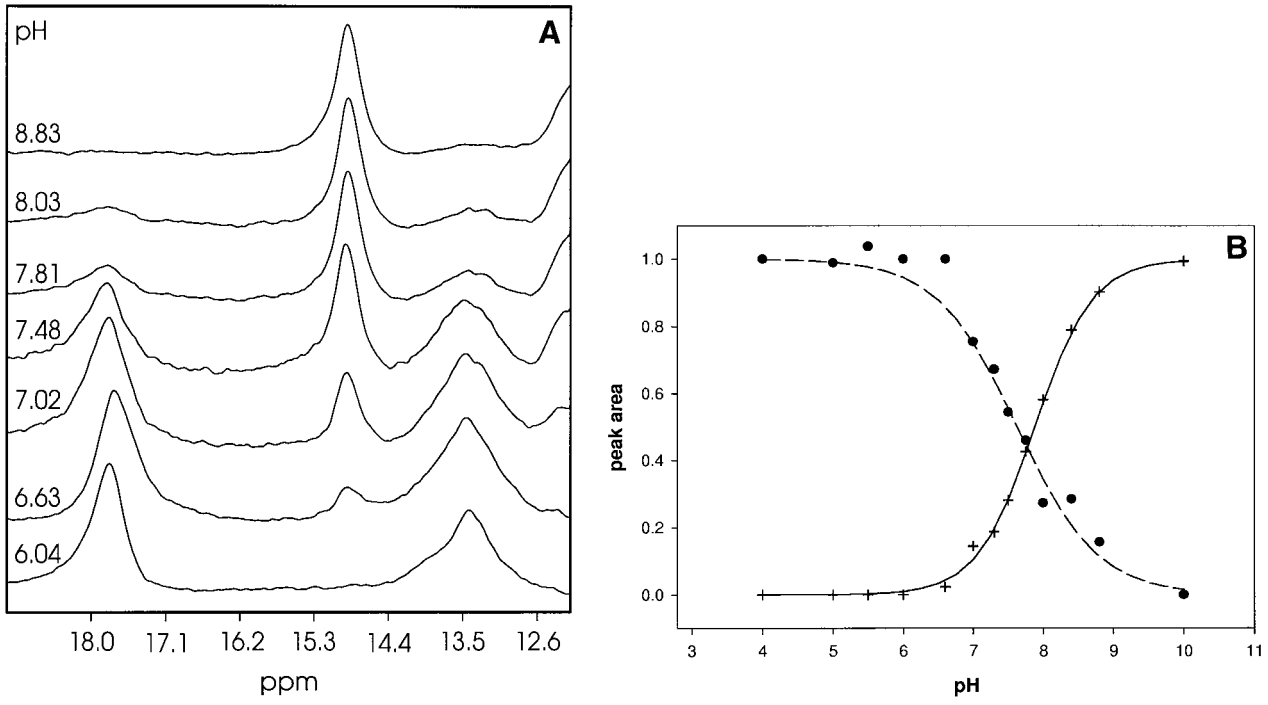

FIG. 1. 750-MHz ^{1}H NMR titration study of rat trypsinogen D189S. (A) High-frequency ^{1}H NMR spectral region at of ~1 mM protein samples at various glass electrode pH meter values indicated in the figure. The protein sample was dissolved in 0.1 M KCl, 95:5% ^1H_2O:^2H_2O. The spectra are the average of 1000 transients collected at 5°C. (B) ^{1}H NMR titration curves from the intensities of both the 17.8 ppm (●) and 14.9 ppm (+) signals from the His^{57} H$^{\delta 1}$. The calculated pK_a values and Hill coefficients are listed in Table I.

by SDS–PAGE (33). The purified human α_1-proteinase inhibitor was contaminated with about 20% active site cleaved inhibitor. Cleaved α_1-proteinase inhibitor was prepared according to the method of Kaslik *et al.* (25). Recombinant rat trypsinogen D189S was produced, purified, and activated as described previously (34). In order to prevent cleavage of the complex by the free enzyme, an excess of inhibitor was added. As determined by SDS–PAGE, the human α_1-proteinase inhibitor:trypsin D189S ratio was 1.1 and the human α_1-proteinase inhibitor:α-chymotrypsin ratio was 2.0. The initial concentration of each enzyme in the solution used for complex formation was about 10–20 μM. The bovine chymotrypsinogen–human α_1-proteinase inhibitor complex was prepared according to the method of Löbermann *et al.* (35). Solutions to be used for NMR spectroscopy were concentrated by ultrafiltration. All solutions were stored at −20°C.

NMR spectroscopy. The approximate protein concentrations in the various samples used for NMR spectroscopy were 1 mM trypsinogen D189S, 1 mM trypsin D189S, 1 mM α-chymotrypsin, 0.4 mM trypsin D189S–α_1-proteinase inhibitor complex, 0.4 mM chymotrypsinogen–α_1-proteinase inhibitor complex, 0.4 mM α-chymotrypsin–α_1-proteinase inhibitor complex, and 1 mM cleaved α_1-proteinase inhibitor. The solvent in each case was 95:5 ^1H_2O:^2H_2O. The pH was measured with a small combination glass electrode, and pH adjustments were made by adding aliquots of 1 or 0.1 M KOH or HCl with rapid stirring. The pH of each sample was checked before and after each spectrum was obtained. ^{1}H NMR data were collected at the National Magnetic Resonance Facility at Madison on Bruker DMX 750 (750 MHz ^{1}H frequency) and DMX 500 (500 MHz ^{1}H frequency) spectrometers (Billerica, MA). A jump and return echo pulse sequence (36), modified for use with pulse field gradients, was used for data acquisition. Spectra were collected at 5°C (or 20°C as noted). Chemical shifts are reported in ppm from the internal reference 2-dimethyl-2-silapentane-5-sulfonate (DSS). Data analysis was performed on Silicon Graphics (Mountain View, CA) workstations with the Felix software package (Biosym, San Diego, CA). The SigmaPlot software package (Sigma) was used for curve fitting.

Exchange rates (k_{ex}) with the solvent of the H$^{\delta 1}$ of His^{57} in the zymogen, active enzyme, and serpin-inhibited forms of trypsin D189S at 5°C at two pH values, pH 5.2 and 10.0, were determined from measurements of the excess linewidth ΔW of the NMR peak assigned to this proton under the slow-exchange approximation, $k_{ex} = \pi\Delta W$. The estimated natural linewidth in the absence of exchange was 43 Hz for the zymogen and the active enzyme species and 137 Hz for α_1-proteinase inhibitor complexes (37). The exchange rates were also measured by following the repopulation of the H$^{\delta 1}$ signal of His^{57} from bulk solvent following selective saturation of the signal according to the equation

$$A_\infty - A = -A_\infty(e^{-k\text{ext}} - 1), \qquad [1]$$

where t is the duration of selective saturation of the His^{57} H$^{\delta 1}$ signal, A_∞ is the total area of His^{57} H$^{\delta 1}$ signal (at t_∞), and A is the area of the repopulated signal from the His^{57} H$^{\delta 1}$ at time t.

RESULTS

Figures 1–3 show the high frequency region of the ^{1}H NMR spectra of the zymogen, active enzyme, and serpin complexed forms of recombinant rat trypsin D189S acquired at different pH values. At pH values well below the pK_a of His^{57}, the ^{1}H NMR spectrum of each form of recombinant rat trypsin D189S exhibited a single peak at about 17.7 ppm. In accordance with data

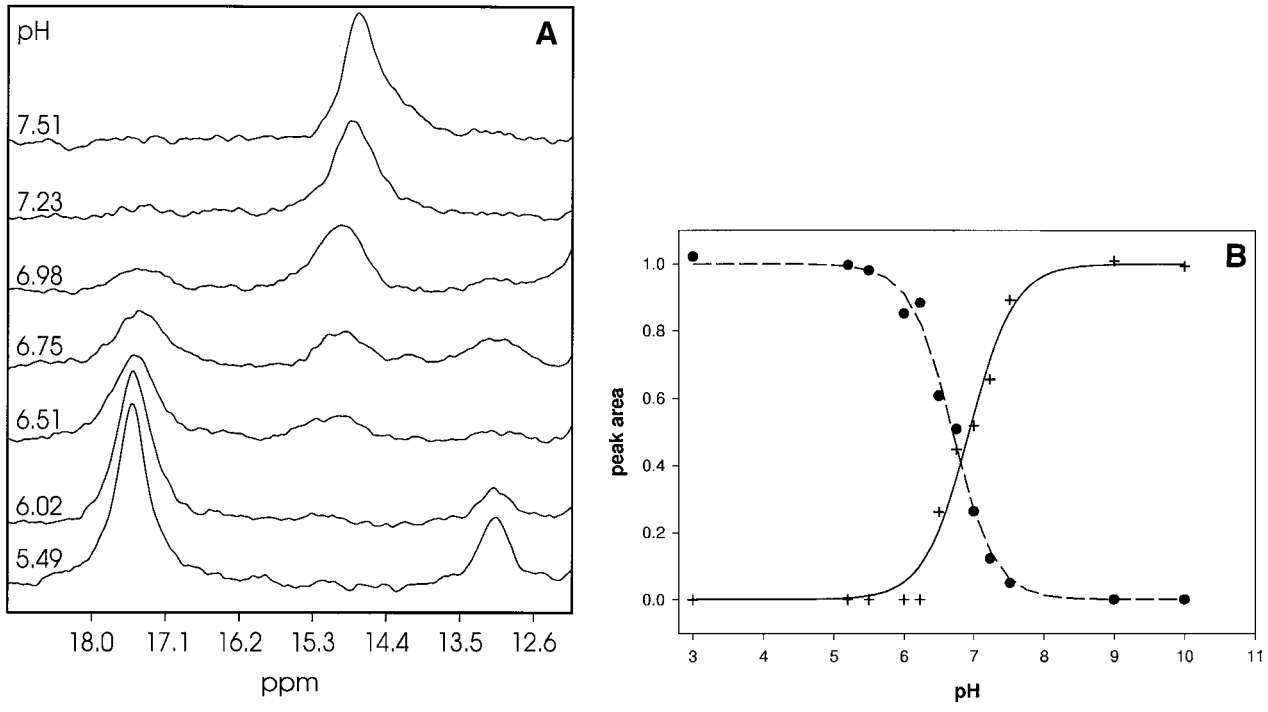

FIG. 2. 500-MHz ^{1}H NMR titration study of rat trypsin D189S. (A) High-frequency ^{1}H NMR spectral region at of ~1 mM protein samples at various glass electrode pH meter values indicated in the figure. The protein sample was dissolved in 0.1 M KCl, 95:5% ^1H_2O:^2H_2O. The spectra are the average of 1000 transients collected at 5°C. (B) ^{1}H NMR titration curves from the intensities of both the 17.7 ppm (●) and 14.7 ppm (+) signals from the His^{57} H$^{\delta 1}$. The calculated pK_a values and Hill coefficients are listed in Table I.

from other serine proteinases (29, 30, 38), this signal was assigned to the H$^{\delta 1}$ proton of His^{57}, which forms the H-bond between positively charged His^{57} and negatively charged Asp^{102} in the active site. As the pH was raised, the 17.7 ppm peak decreased in intensity, and a peak at about 14.8 ppm grew in; the latter peak was assigned to the same H$^{\delta 1}$ proton in protein with neutral His^{57}.

The experimentally determined areas of the peaks at 17.7 and 14.8 ppm, as a function of pH for each of the three forms of rat trypsin D189S, served as input for calculations of the titration parameters. The pK_a values of His^{57} calculated independently from each of the two peaks were found to be very similar. The calculated titration curves for each are compared with the experimental data points in Figs. 1B, 2B, and 3B. The determined pK_a values and Hill coefficients are summarized in Table I. Activation of the zymogen was found to affect both the pK_a value of His^{57} and the cooperativity of proton binding. In the zymogen, the pK_a of His^{57} is 7.8, and proton binding shows weak negative cooperativity (n = 0.86); in the active enzyme, the pK_a of His^{57} is lowered by 1.1 units to 6.7, and proton binding shows weak positive cooperativity (n = 1.37). In the complex between rat trypsin D189S and human α_1-proteinase inhibitor, the pK_a of His^{57} is 8.1, and proton binding shows weak negative cooperativity (n = 0.70); these properties are similar to those of His^{57} in the zymogen (Table I).

Rates of exchange of the His^{57} H$^{\delta 1}$ proton with bulk solvent were determined in two ways: first, from the linewidth of the ^{1}H NMR signal in excess of that expected in the absence of exchange, and second, from the rate of repopulation of the site by protons from bulk solvent following selective saturation of the signal (Fig. 4). Exchange rates were determined for the His^{57} H$^{\delta 1}$ at two pH values (pH 5.2 and pH 10.0) for the zymogen, active enzyme, and serpin complexed forms of trypsin D189S. The rates determined by the two methods (Table I) were equivalent within experimental error (with one exception, trypsin D189S at pH 10, where the measured exchange rates differed by less than a factor of 2). Comparison of the exchange rates from the three forms of trypsin D189S indicated no appreciable difference in the solvent exposure of the Asp^{102}–His^{57} catalytic dyad and confirmed that it is not disrupted in the serpin complex.

The comparative effects of complex formation with human α_1-proteinase inhibitor on the environments of His^{57} H$^{\delta 1}$ of bovine chymotrypsinogen, bovine α-chymotrypsin, and rat trypsin D189S are shown in Figs. 5–7. The ^{1}H NMR spectra of uncomplexed bovine α-chymotrypsin (Fig. 6A) and uncomplexed bovine chymotrypsinogen (Fig. 7A) showed peaks previously assigned to

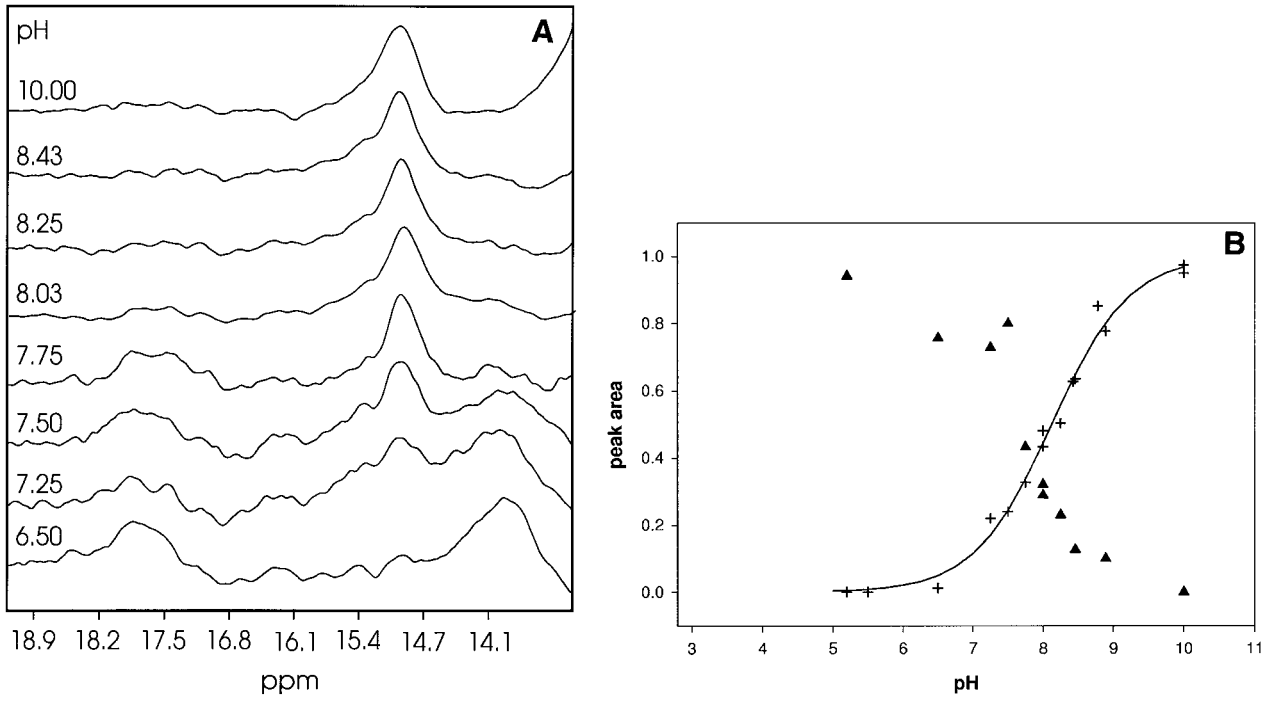

FIG. 3. 500-MHz ^{1}H NMR pH titration study of the rat trypsin D189S–α_1-proteinase inhibitor complex. (A) High-frequency ^{1}H NMR spectral region at of ~0.4 mM protein samples at various glass electrode pH meter values indicated in the figure. The protein sample was dissolved in 0.1 M KCl, 95:5% ^1H_2O:^2H_2O. The spectra are the average of 1000 transients collected at 5°C. (B) ^{1}H NMR titration curves of the His^{57} H$^{\delta 1}$ peaks. The intensities of both the 17.7 ppm (▲) and 14.8 ppm (+) signals are shown, but a pK_a value was derived only from the 14.8 ppm peak, because the 17.7 ppm peak was too broad for accurate intensity measurements. The calculated pK_a values and Hill coefficients are listed in Table I.

His^{57} H$^{\delta 1}$ (28, 29) with chemical shifts of 15.0 ppm at pH 10.0 and at 18.0 ppm at pH 5.2, at both 5 and 20ºC. Whereas in α-chymotrypsin the peak at 18 ppm (at pH 5.2) had a similar width at 20 and 5ºC (Fig. 6A, cd), in chymotrypsinogen the peak at this position (18 ppm) was significantly broader at 20ºC than at 5ºC (Fig. 7A, cd). At pH 5.2, an additional temperature-dependent peak was observed at 13.2 ppm; this peak was sharper at both temperatures in spectra of the zymogen (Fig. 7A, ab) than in those of the enzyme (Fig. 6A, ab). Peaks at similar chemical shifts were seen in spectra of the bovine α-chymotrypsin–human α_1-proteinase inhibitor complex (Fig. 6B) and bovine chymotrypsinogen–human α_1-proteinase inhibitor complex (Fig. 7B); however, the peaks were much broader than those of the uncomplexed proteins, and the linewidths exhibited a

TABLE I

^{1}H NMR-Derived Parameters for His^{57} of Rat Trypsinogen D189S, Trypsin D189S, and Trypsin D189S–α_1-Proteinase Inhibitor Complex at 5°C

	Titration parameters		H$^{\delta 1}$ signal of His^{57} at pH 5.2			H$^{\delta 1}$ signal of His^{57} at pH 10.0		
Protein species	pK_a of His^{57}	Hill coefficient[a]	Chemical shift (ppm)	Exchange rate; from linewidth (s^{-1})	Exchange rate; from recovery (s^{-1})	Chemical shift (ppm)	Exchange rate; from linewidth (s^{-1})	Exchange rate; from recovery (s^{-1})
Trypsinogen D189S	7.8 ± 0.1	0.86 ± 0.05	17.8	470 ± 80	410 ± 70	14.9	210 ± 50	250 ± 70
Trypsin D189S	6.7 ± 0.1	1.37 ± 0.08	17.7	370 ± 70	280 ± 50	14.7	520 ± 90	290 ± 30
Trypsin D189S–α_1-proteinase inhibitor complex	8.1 ± 0.1	0.70 ± 0.08	17.7	380 ± 100	600 ± 250	14.8	140 ± 40	80 ± 30

[a] A measure of cooperativity of the transition.

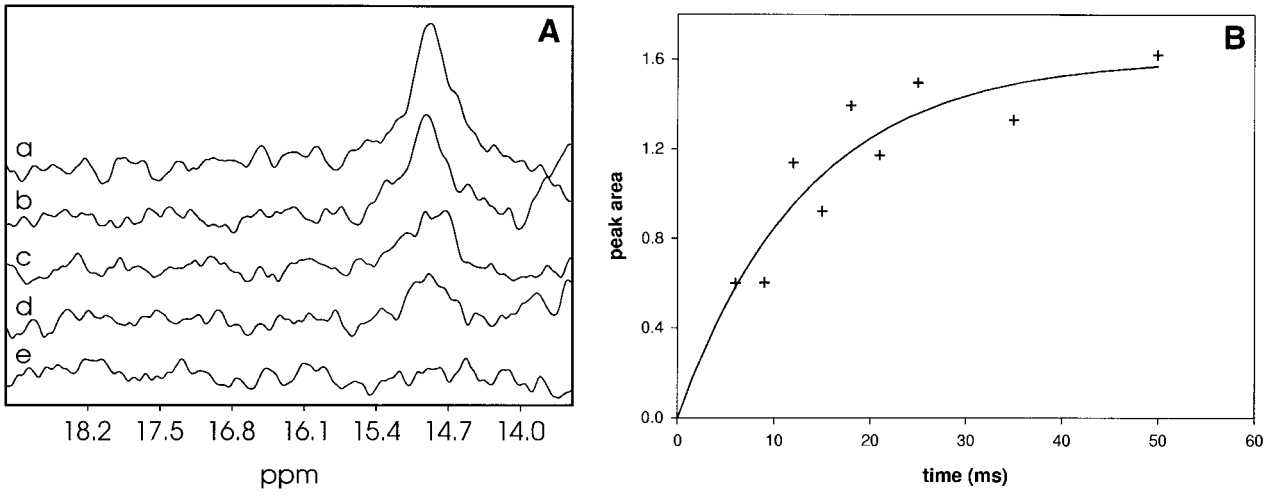

FIG. 4. Measurement by 500-MHz ^{1}H NMR spectroscopy of the solvent exchange off rate of His^{57} H$^{\delta 1}$ of the trypsin D189S–α_1-proteinase inhibitor complex at pH 10.0 and 5°C. (A) Repopulation by exchange from bulk solvent of the His^{57} H$^{\delta 1}$ signal following different delay times inserted into the pulse sequence between the selective saturation of the signal and the jump and return echo. The delay times are shown in the figure. The sample was ~0.4 mM complex dissolved in 0.1 M KCl, 95:5% ^1H_2O:^2H_2O. (B) Plot of ^{1}H NMR signal area (A) as a function of the delay time (t) according to the equation: $A_\infty - A = -A_\infty(e^{-kext} - 1)$, where t is the time following the selective saturation of the His^{57} H$^{\delta 1}$ signal, A_∞ is the total area of the His^{57} H$^{\delta 1}$ signal (at t_∞), and A is the area of the repopulated His^{57} H$^{\delta 1}$ signal at t. The calculated exchange off rates are listed in Table I.

much stronger temperature dependence. Broad peaks at 18 ppm at pH 5.2 were resolved at 5ºC, but not at 20ºC in the spectra of the bovine α-chymotrypsin–human α_1-proteinase inhibitor complex (Fig. 6B, cd) and the bovine chymotrypsinogen–human α_1-proteinase inhibitor complex (Fig. 7B, cd). Whereas in the free

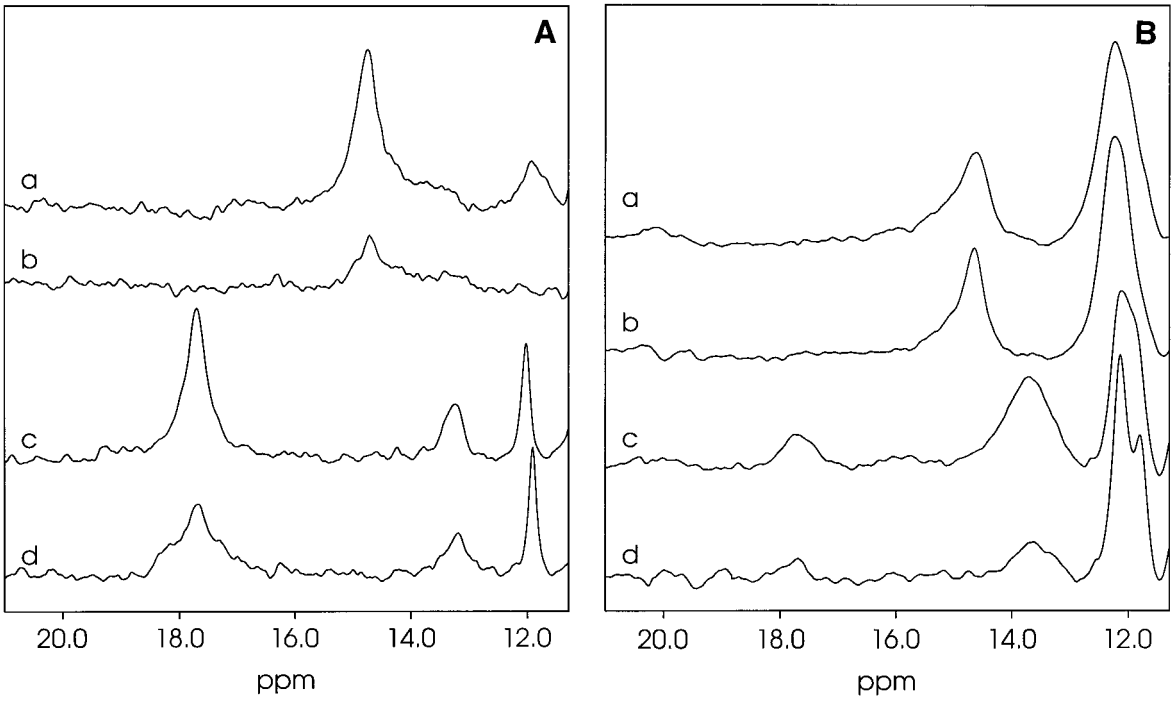

FIG. 5. High-frequency region of 500-MHz ^{1}H NMR spectra of (A) rat trypsin D189S, (B) trypsin D189S–α_1-proteinase inhibitor complex. The spectra represent 1000 transients collected at (a) pH 10.0 at 5°C; (b) pH 10.0 at 20°C; (c) pH 5.2 at 5°C; (d) pH 5.2 at 20°C. The concentrations of the samples were ~1 mM for trypsin D189S and ~0.4 mM for the complex. The samples were dissolved in 0.1 M KCl, 95:5% ^1H_2O:^2H_2O.

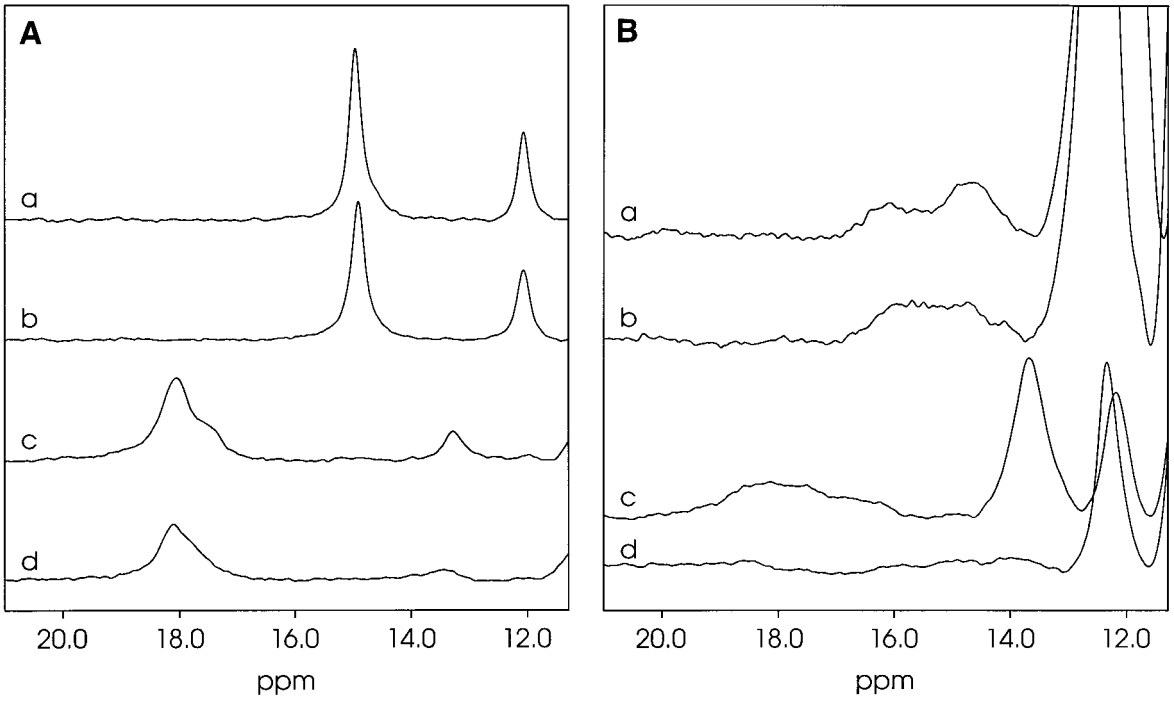

FIG. 6. High-frequency region of 500-MHz ^{1}H NMR spectra of (A) bovine α-chymotrypsin (1000 transients) and (B) bovine α-chymotrypsin–α_1-proteinase inhibitor complex (10,000 transients). The spectra were collected at (a) pH 10.0 at 5°C; (b) pH 10.0 at 20°C; (c) pH 5.2 at 5°C; (d) pH 5.2 at 20°C. The concentrations of the samples were ~1 mM for α-chymotrypsin and ~0.4 mM for the complex. The samples were dissolved in 0.1 M KCl, 95:5% ^1H_2O:^2H_2O.

enzymes, trypsin D189S (Fig. 5A), and α-chymotrypsin (Fig. 6A), the peak at 18.0 ppm was sharper or more intense than that at 13.2 ppm, in the zymogens, trypsinogen D189S (Fig. 1A) and chymotrypsinogen (Fig. 7A, cd), and each serpin complex (Figs. 5B, cd; 6B, cd; and 7B, cd), the peaks appearing at 18 ppm were broader than that at 13.7 ppm. At high pH (pH 10.0) a signal in the position expected for His^{57} H$^{\delta 1}$ was observed in spectra of both the bovine α-chymotrypsin–human α_1-proteinase inhibitor complex (Fig. 6B, ab) and the bovine chymotrypsinogen–human α_1-proteinase inhibitor complex (Fig. 7B, ab). This signal was relatively sharp at both 5 and 20°C in the spectra of chymotrypsinogen complex (Fig. 7B, ab), and, as with free chymotrypsinogen (Fig. 7A, ab), it showed a slight downfield shift at higher temperature. In the bovine chymotrypsin–human α_1-proteinase inhibitor complex, this signal appeared to be split at 5°C (Fig. 6B, a), but the components were broadened and closer together at 20°C (Fig. 6B, b). This suggests that His^{57} may exist in two interconverting conformational states in this complex, a result not observed with the bovine chymotrypsinogen–human α_1-proteinase inhibitor complex nor with the rat trypsin D189S–human α_1-proteinase inhibitor complex.

^{1}H NMR spectra of the cleaved form of human α_1-proteinase inhibitor were acquired under similar conditions: pH 10 at 5°C (Fig. 8a) and 20°C (Fig. 8b) and pH 5.2 at 5°C (Fig. 8c) and 20°C (Fig. 8d). As expected, these spectra showed no peaks in the region of the signals assigned to His^{57} H$^{\delta 1}$ of the proteinases. The cleaved inhibitor at pH 5.2 and 5°C (Fig. 8c) showed a peak at 13.7 ppm that became severely broadened at 20°C (Fig. 8d). A peak in this position was not observed in similar spectra of the intact inhibitor (spectra not shown). Peaks at this position and with similar (but less severe) temperature-dependent linewidths were observed in spectra of the three complexes (Figs. 5–7). These peaks thus can be attributed to the cleaved form of the inhibitor.

DISCUSSION

Previous attempts at using ^{1}H NMR to investigate the state of His^{57} in serpin–proteinase complexes yielded contradictory results. The failure to observe a signal from the His^{57} H$^{\delta 1}$ in the bovine α-chymotrypsin–recombinant human α_1-antichymotrypsin variant complex (26) was interpreted as indicative of disruption of the Asp^{102}–His^{57} dyad in that complex. Observation, however, of a signal attributed to the His^{57} H$^{\delta 1}$ in the rat trypsin D189S–human α_1-proteinase inhibitor complex with an apparent pK_a higher than that of the free proteinase was interpreted as indicating that

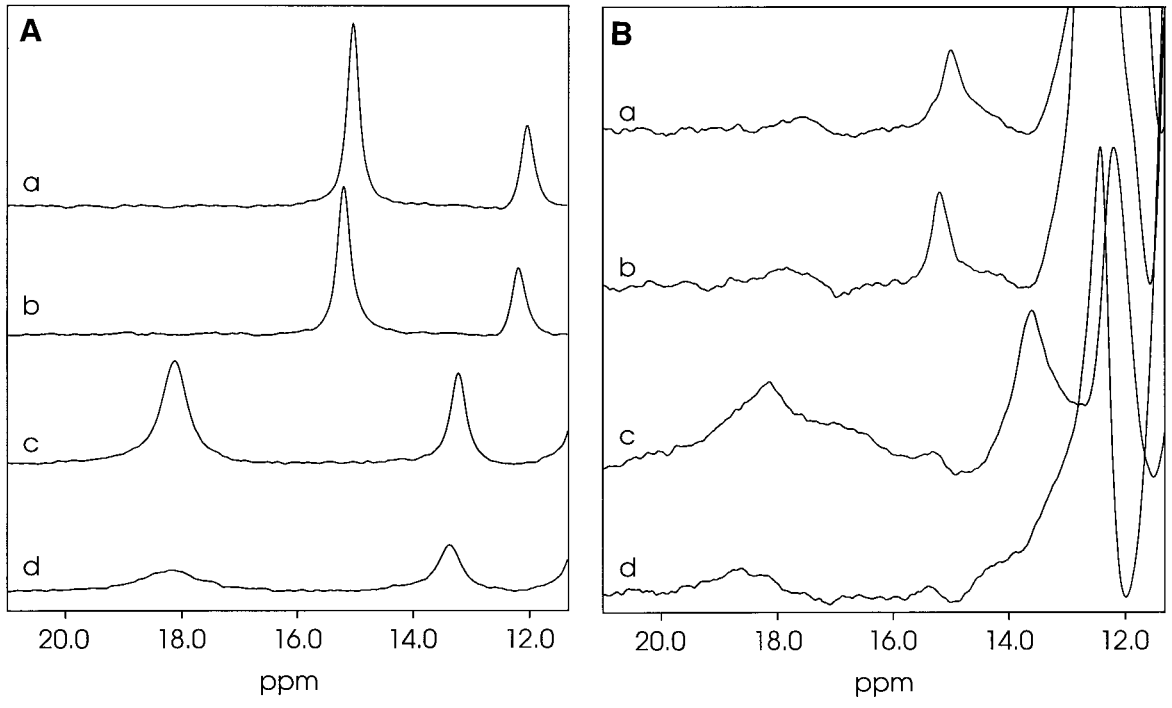

FIG. 7. High-frequency region of 500-MHz ^{1}H NMR spectra of (A) bovine chymotrypsinogen (1000 transients) and (B) bovine α-chymotrypsinogen–α_1-proteinase inhibitor complex (10,000 transients). The spectra were collected at (a) pH 10.0 at 5°C; (b) pH 10.0 at 20°C; (c) pH 5.2 at 5°C; (d) pH 5.2 at 20°C. The concentrations of the samples were ~1 mM for chymotrypsinogen and ~0.4 mM for the complex. The samples were dissolved in 0.1 M KCl, 95:5% ^1H_2O:^2H_2O.

the Asp^{102}–His^{57} dyad is intact in the complex and that the pK_a of His^{57} is perturbed upward in the complex. Full resolution of these contradictory results is of importance because they may provide useful information on the mechanism responsible for the longevity of the complex, which resembles an acyl-enzyme intermediate. One experiment suggested that the catalytic apparatus becomes inactivated on complex formation by disruption of the critical His^{57}–Asp^{102} hydrogen bond (26); the other suggested that the enzyme is inactivated by structural rearrangement around the active site and by stabilization of the protonated state of the catalytic histidine (25). The deprotonated form of the imidazole is responsible for extracting a proton from the water molecule that attacks the acyl-enzyme. A similar mechanism is thought to contribute (30), along with differences in the structure of the specificity pocket (27), to the decreased activities of chymotrypsinogen and trypsinogen relative to their active states.

The present investigation confirms the observation of a high-frequency signal from His^{57} H$^{\delta 1}$ in the rat trypsin D189S–human α_1-proteinase inhibitor complex and shows the presence of a similar peak in the ^{1}H NMR spectra of the bovine chymotrypsinogen–human α_1-proteinase inhibitor (Fig. 7B) and bovine α-chymotrypsin–human α_1-proteinase inhibitor complexes (Fig. 6B). ^{1}H NMR spectra of the cleaved form of human α_1-proteinase inhibitor (Fig. 8) had no peaks in the region of those assigned to His^{57} H$^{\delta 1}$ in the proteinases; however, the spectra revealed a peak at 13.7 ppm, which was relatively sharp peak at 5°C but broadened at 20°C. The similar peak observed in spectra of the serpin complexes (Figs. 5B, 6B, and 7B) probably arises from this group in the inhibitor.

Plotnick *et al.* (26) observed the characteristic high-frequency signal of His^{57} H$^{\delta 1}$ in bovine α-chymotrypsin and its complexes with canonical inhibitors, such as BPTI and STI. Their failure to observe a signal from His^{57} in ^{1}H NMR spectra of the complex between bovine chymotrypsin and a recombinant human α_1-antichymotrypsin variant may simply have resulted from the fact that their data were collected at 25°C and at 500 MHz, under conditions where our results with the bovine α-chymotrypsin–human α_1-proteinase inhibitor complex showed no signal at low pH or a broad signal at high pH (Fig. 6B). Another factor that should be taken into consideration is the degree of proteolytic modification of the complexed chymotrypsin. Chymotrypsin has increased sensitivity to proteolysis in the complex (24), and limited proteolysis could have led to an increase in the exchange rate of the N–H proton of His^{57}.

The present studies have provided pH titration parameters for His^{57} of rat trypsin D189S in three states:

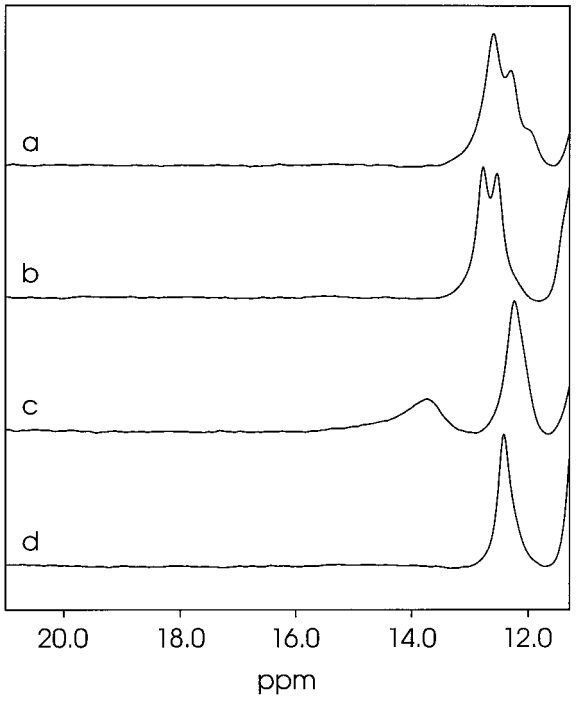

FIG. 8. High-frequency region of 500-MHz ^1H NMR spectra of cleaved α_1-proteinase inhibitor. The spectra are the averages of 1000 transients collected at (a) pH 10.0 at 5°C; (b) pH 10.0 at 20°C; (c) pH 5.2 at 5°C; (d) pH 5.2 at 20°C. The concentrations of the sample was about 1 mM. The sample was dissolved in 0.1 M KCl, 95:5% ^1H_2O: ^2H_2O.

the zymogen, the active enzyme, and the complex with human α_1-proteinase inhibitor (Table I). The results indicate that the pK_a of the active enzyme (pK_a = 6.7) is lower than those of the zymogen (pK_a = 7.8) and serpin complex (pK_a = 8.1). Thus formation of the trypsin D189S–α_1-proteinase inhibitor complex increases the pK_a of His^{57} by about 1 unit. By contrast, complex formation of serine-proteinases with canonical inhibitors lowers the pK_a dramatically. For example, the pK_a of His^{57} was calculated to be 3.0–3.5 in the bovine α-chymotrypsin–BPTI and porcine trypsin–BPTI complexes (32). The exchange off rates of His^{57} $H^{\delta 1}$ of trypsin D189S in its zymogen, active, and α_1-proteinase inhibitor complex are all with values of 2–12.5 ms. In the canonical inhibitor–serine proteinase complexes, however, the ^1H NMR signal of His^{57} $H^{\delta 1}$ becomes sharper; i.e., the lifetime of the His^{57} $H^{\delta 1}$ is longer in the complex than in the uncomplexed proteinase (30, 26). For example, in free bovine α-chymotrypsin, the lifetime of the His^{57} $H^{\delta 1}$ was measured to be $<$10 ms, whereas in the α-chymotrypsin–BPTI complex the lifetime of the same proton was $>$1 s (26). These observations further support the view that serpins and canonical inhibitors interact with serine proteinases in markedly different ways.

Differences were also observed in the slopes of the titration curves for the three forms of trypsin D189S: the protonation at His^{57} $N^{\epsilon 2}$ in active rat trypsin D189S showed significant positive cooperativity (n = 1.37), whereas both in the zymogen (n = 0.86) and serpin complex (n = 0.70) the protonation step showed slight negative cooperativity. Analogous results have been seen for bovine α-chymotrypsin (n = 1.35) and bovine chymotrypsinogen (n = 0.96) (32). The structural differences between the zymogen and the active enzyme may be analogous to those between the complex and the active enzyme. Conversion of the zymogen to the active enzyme is initiated by proteolytic cleavage at the N-terminus of the molecule; this leads to a structural rearrangement in a defined part of the proteinase, called the activation domain (residues in trypsin: 16–19, 142–152, 184–194, and 216–224; (27)). In the zymogen, the activation domain is improperly folded and usually less ordered than in the activated enzyme. The catalytic serine is located on the border of the activation domain, whereas the oxyanion hole and the substrate-binding pocket are integral to the activation domain. The catalytic triad is already formed in the zymogen and appears not to undergo a structural rearrangement in the activation process, although the chemical properties of the catalytic histidine (pK_a, Hill coefficient) are changed. The mechanism behind these changes is not clearly understood.

The properties of His^{57} in the trypsin D189S–α_1-proteinase inhibitor complex resemble those of the zymogen, rather than those of the active enzyme. The changes of pK_a and Hill coefficients ongoing from the active enzyme to the complex are in the same direction but larger than those between the active enzyme and zymogen. The mechanism responsible for the altered pK_a of His^{57} in the serpin complex is of major interest. Factors to be considered are the effect of acylation of Ser^{195} and those of conformational alterations. NMR data are available for one acyl enzyme complex: in this study, acylation of bovine α-chymotrypsin with *p*-nitrophenyl N^2-(*N*-acetylalanyl)-N^1-benzyl carbazoate lowered the pK_a value from 7.5 to 6.5 (28). The pH dependence of deacylation reaction kinetics suggests that the pK_a of His^{57} in the acyl-enzyme intermediate is about 7 (39). By contrast to the effects of acylation, which lower the pK_a of His^{57}, disordering of the activation domain to a zymogen-like structure, which has been postulated to occur on serpin binding (7, 25), appear to raise the pK_a of His^{57}. In the three zymogen/enzyme pairs studied to date, the pK_a of His^{57} in the zymogen has been higher than that in the enzyme; the amount of the difference has varied between 0.5 pH units for bovine chymotrypsinogen/α-chymotrypsin (30, 32), to 1.1 units for rat trypsinogen D189S/trypsin D189S (present studies), to 2.7 pH units for porcine trypsinogen/trypsin (31, 40). The α_1-proteinase inhibitor induced conformational

change of trypsin D189S (7, 25) is probably initiated through the acyl-linkage formed between the Met^{358} residue of the inhibitor and the Ser^{195} residue of the enzyme. This structural change could have an effect on the peptide chain conformation around the catalytic serine, where the oxyanion hole and one part of the binding pocket are located, and may induce rearrangement of the plastic activation domain leading to changes in the properties of His^{57}.

The significant difference between the activation domain structure of rat trypsin and bovine α-chymotrypsin might explain the observed difference in the linewidths of the ^1H NMR signals from His^{57} $H^{\delta 1}$ in their serpin complexes. The activation domain of trypsin remains intact following zymogen activation, whereas that of bovine α-chymotrypsin loses a dipeptide as the result of autolytic cleavage at Tyr^{146} and Asn^{148}. Deletion of the dipeptide makes the 142–152 loop more flexible and probably makes the whole activation domain more vulnerable to serpin-induced structural change. This model is supported by the observation here of sharper signals in spectra of the bovine chymotrypsinogen–human α_1-proteinase inhibitor complex (Fig. 7B), where the activation domain of the chymotrypsinogen is intact, than in the bovine α-chymotrypsin–human α_1-proteinase inhibitor complex (Fig. 6B), where cleavage and loss of the dipeptide have occurred. Thus residues in the activation domain of bovine chymotrypsin may undergo a larger conformational change during the complex formation with α_1-proteinase inhibitor than those of trypsin D189S and chymotrypsinogen . This would explain the faster exchange rate (broader line) of His^{57} $H^{\delta 1}$ in the former complex than the latter ones.

What role do enzyme–substrate interactions play in the stabilization and breakdown of the acyl-enzyme state? Ding *et al.* (41), who used X-ray crystallographic cryoenzymology to investigate the structure of an acyl-enzyme intermediate, observed that $N^{\epsilon 2}$ of His^{57} forms a hydrogen bond with O^{γ} of Ser^{195} in the frozen acyl-enzyme intermediate and that the substrate P_1 carbonyl oxygen occupies the oxyanion hole within hydrogen-bonding distance from the main chain nitrogens of both Gly^{193} and Ser^{195}. It was also reported that the P_1 side chain, surprisingly, did not interact with the binding pocket. In accord with this observation, the deacylation rate was found to be independent of the substrate length and the identity of the side chain at P_1 (42). Thus, among the various enzyme–substrate interactions, only the covalent bond between O^{γ} of Ser^{195} and the substrate P_1 carbonyl carbon and the hydrogen bonds in the oxyanion hole seem to play important roles in the stabilization and decomposition of the acyl-enzyme intermediate. Interactions at $P_{1,2,3,\ldots}$–$S_{1,2,3,\ldots}$ sites, however, make no significant contribution to the breakdown of the acyl-enzyme state.

Several lines of evidence suggest that the structural changes induced by the formation of the serpin complex resemble in reverse those that accompany zymogen activation. Considering that the deacylation reaction is dependent primarily on the properties of the catalytic triad and the conformation of the oxyanion hole, longevity of the serpin complex can be achieved by changes of the structure of these elements alone. A small change in the conformation of Ser^{195} and disruption of oxyanion hole can lead to complete loss of enzyme activity. Changing the Ser^{195} conformation and its interaction with His^{57} could also have an effect on the pK_a of His^{57} explaining the upward shift of its pK_a in the complex.

REFERENCES

1. Laskowski, M. J., and Kato, I (1980) *Annu. Rev. Biochem.* **49,** 593–626.
2. Baillargeon, M. W., Laskowski, Jr., M., Neves, D. E., Porubcan, M. A., Santini, R. E., and Markley, J. L. (1980) *Biochemistry* **19,** 5703–5710.
3. Richarz, R., Tschesche, and Wüthrich, K. (1980) *Biochemistry* **19,** 5711–5715.
4. Wagner, G., Braun, W., Havel, T. F., Schaumann, T., Go, N., and Wüthrich, K. (1987) *J. Mol. Biol.* **196,** 611–641.
5. Krezel, A. M., Darba, P., Robertson, A. D., Fejzo, J., Macura, S., and Markley, J. L. (1994) *J. Mol. Biol.* **242,** 203–214.
6. Shore, J. D., Day, D. E., Francis-Chmura, A. M., Verhamme, I. M., Kvassman, J. O., Lawrence, D. A., and Ginsburg, D. (1995) *J. Biol. Chem.* **270,** 5395–5398.
7. Kaslik, G., Patthy, A., Bálint, M., and Gráf, L. (1995) *FEBS Lett.* **370,** 179–183.
8. Lawrence, D. A., Ginsburg, D., Day, D. E., Berkenpas, M. B., Verhamme, I. M., Kvassman, J. O., and Shore, J. D. (1995) *J. Biol. Chem.* **270,** 25309–25312.
9. Wilczynska, M., Fa, M., Ohlsson, P. I., and Ny, T. (1995) *J. Biol. Chem.* **270,** 29652–29655.
10. Engh, R., Huber, R., Bode, W., and Schulze, A. J. (1995) *Trends Biotechnol.* **13,** 503–510.
11. Schechter, I., and Berger, A. (1967) *Biochem. Biophys. Res. Commun.* **27,** 157–162.
12. Stein, P., and Chothia, C. (1991) *J. Mol. Biol.* **221,** 615–621.
13. Carrell, R. W., Stein, P. E., Fermi, G., and Wardell, M. R. (1994) *Structure* **2,** 257–270.
14. Schreuder, H. A., de Boer, B., Dijkema, R., Mulders, J., Theunissen, H. J. M., Grootenhuis, P. D. J., and Hol, W. G. J. (1994) *Nature Struct. Biol.* **1,** 48–54.
15. Wei, A., Rubin, H., Cooperman, B. S., and Christianson, D. W. (1994) *Nature Struct. Biol.* **1,** 251–258.
16. Song, H. K., Lee, K. N., Kwon, K. S., Yu, M. H., and Suh, S. W. (1995) *FEBS Lett.* **377,** 150–154.
17. Elliott, P. R., Lomas, D. A., Carrell, R. W., and Abrahams, J. P. (1996) *Nature Struct. Biol.* **3,** 676–681.
18. Bode, W., and Huber, R. (1992) *Eur. J. Biochem.* **204,** 433–451.
19. Löbermann, H., Tokuoka, R., Deisenhofer, J., and Huber, R. (1984) *J. Mol. Biol.* **177,** 531–556.
20. Baumann, U., Huber, R., Bode, W., Grosse, D., Lesjak, M., and Laurell, C. B. (1991) *J. Mol. Biol.* **218,** 595–606.

21. Mourey, L., Samama, J.-P., Delaure, M., Petitou, M., Choay, J., and Moras, D. (1993) *J. Mol. Biol.* **232,** 223–241.
22. Aertgeerts, K., De-Bondt, H. L., De-Ranter, C., and Declerck, P. J. (1995) *Proteins* **23,** 118–121.
23. Potempa, J., Korzus, E., and Travis, J. (1994) *J. Biol. Chem.* **269,** 15957–15960.
24. Stavridi, E. S., O'Malley, K., Lukacs, C. M., Moore, W. T., Lambris, J. D., Christianson, D. W., Rubin, H., and Cooperman, B. S. (1996) *Biochemistry* **35,** 10608–10615.
25. Kaslik, G., Kardos, J., Szabó, E., Szilágyi, L., Závodszky, P., Westler, W. M., Markley, J. L., and Gráf, L. (1997) *Biochemistry* **36,** 5455–5464.
26. Plotnick, M. I., Mayne, L., Schechter, N. M., and Rubin, H. (1996) *Biochemistry* **35,** 7586–7590.
27. Huber, R., and Bode, W. (1978) *Acc. Chem. Res.* **11,** 14–122.
28. Robillard, G., and Shulman, R. G. (1972) *J. Mol. Biol.* **71,** 507–511.
29. Robillard, G., and Shulman, R. G. (1974) *J. Mol. Biol.* **86,** 519–540.
30. Markley, J. L. (1978) *Biochemistry* **17,** 4648–4656.
31. Porubcan, M. A., Neves, D. E., Rausch, S. K., and Markley, J. L. (1978) *Biochemistry* **17,** 4640–4647.
32. Markley, J. L., and Ibañez, I. B., (1978) *Biochemistry* **17,** 4627–4640.
33. Laemmli, U. K. (1970) *Nature* **227,** 680–685.
34. Gráf, L., Jancsó, A., Szilágyi, L., Hegyi, G., Pintér, K., Náray-Szabó, G., Hepp, J., Medzihradszky, K., and Rutter, W. J. (1988) *Proc. Natl. Acad. Sci. USA* **85,** 4961–4965.
35. Löbermann, H., Lottspeich, F., Bode, W., and Huber, R. (1982) *Hoppe-Seyler's Z. Physiol. Chem.* **363.** 1377–1388.
36. Sklenár, V., and Bax, A. (1987) *J. Magn. Reson.* **74,** 469–479.
37. Ash, E. L., Sudmeier, J. L., De Fabo, E. C., and Bachovchin, W. W. (1997) *Science* **278,** 1128–1132.
38. Markley J. L., and Westler, W. M. (1996) *Biochemistry* **35,** 11092–11097.
39. Amshey, J. W., Jr., Jindal, S. P., and Bender, M. L. (1975) *Arch. Biochem. Biophys.* **169,** 1–6.
40. Markley, J. L., and Porubcan, M. A., (1976) *J. Mol. Biol.* **102,** 487–509.
41. Ding, X., Rasmussen, B. F., Petsko, G. A., and Ringe, D. (1994) *Biochemistry* **33,** 9285–9293.
42. Hedstrom, L., Szilágyi, L., and Rutter W. J. (1992) *Science* **255,** 1249–1253.